Magmatic history of the northeastern Tibetan Plateau

George E. Gehrels
Department of Geosciences, University of Arizona, Tucson, Arizona, USA

An Yin
Department of Earth and Space Sciences, University of California, Los Angeles, California, USA

Xiao-Feng Wang
Chinese Academy of Geological Sciences, Institute of Geomechanics, Beijing, China

Received 13 March 2002; revised 4 January 2003; accepted 16 January 2003; published 12 September 2003.

[1] The northeastern margin of the Tibetan Plateau is underlain by the Qaidam and Qilian terranes, which consist primarily of mid-Proterozoic through lower Paleozoic oceanic and arc-type assemblages that have been accreted to the southern margin of the Tarim/Sino-Korean craton. Most previous models suggest that these assemblages formed along a northeast dipping subduction system constructed along the margin of the Tarim/Sino-Korean craton during early Paleozoic time. The main components are interpreted to have formed either as an archipelago of volcanic arcs and back arc basins, or as a broad expanse of accretionary complexes. Our geochronologic data support a model, suggested by *Sobel and Arnaud* [1999], in which the Qaidam and Qilian terranes are separated from the Tarim/Sino-Korean craton by a mid-Paleozoic suture that closed along a southwest dipping subduction zone. The basement to these terranes consists of oceanic assemblages that were amalgamated into a coherent crustal fragment prior to emplacement of ~920–930 Ma granitoids. Early Paleozoic arc-type magmatism occurred between ~480 and ~425 Ma, apparently sweeping southwestward across much of the Qilian and Qaidam terranes. Accretion-related magmatism along the inboard margin of the Qilian terrane occurred between ~423 Ma and ~406 Ma. Following Silurian-Devonian accretion, the region has experienced late Paleozoic and Mesozoic uplift and erosion and has been severely overprinted by Tertiary thrusting, uplift, and strike-slip motion along the Altyn Tagh fault. Correlation of geologic features and magmatic histories between the Altun Shan and the Nan Shan suggests that the eastern Altyn Tagh fault has a total left-lateral offset of ~375 km. *INDEX TERMS:* 8105 Tectonophysics: Continental margins and sedimentary basins (1212); 8110 Tectonophysics: Continental tectonics—general (0905); 8125 Tectonophysics: Evolution of the Earth; 8157 Tectonophysics: Plate motions—past (3040); *KEYWORDS:* tectonics, China, Tibet, Paleozoic magmatism

Citation: Gehrels, G. E., A. Yin, and X.-F. Wang, Magmatic history of the northeastern Tibetan Plateau, *J. Geophys. Res.*, *108*(B9), 2423, doi:10.1029/2002JB001876, 2003.

1. Introduction

[2] The northeastern portion of the Tibetan Plateau contains a variety of crustal fragments that have been accreted to the southern margin of the Tarim/Sino-Korean craton (Figure 1). The cratonal regions northeast of the plateau consist largely of Precambrian crystalline basement, overlain locally by Proterozoic, Paleozoic, and Mesozoic platformal strata [*Liu*, 1988; *Yin and Harrison*, 2000]. These rocks generally occur at elevations of <2 km with low topographic relief and little sign of active deformation (Figure 1). To the south and west of the cratons is a collage of arc-type, ocean floor, and shallow marine assemblages, referred to as the Qilian and Qaidam terranes [*Yin and Harrison*, 2000], which are exposed in the Altun Shan, Nan Shan, and Qilian Shan (Figure 1). These mountainous regions are underlain largely by accreted rocks of mid-Proterozoic to mid-Paleozoic age, Devonian through Cretaceous marine and continental platformal strata, and Tertiary synorogenic deposits. Figure 2 shows the distribution of the main assemblages in the area and provides a brief description of their lithotectonic constituents.

[3] An additional element in the region is the Qaidam basin, which is a low-relief basinal terrane within the northeastern Tibetan Plateau (Figure 1). Many workers have suggested that the Qaidam terrane is underlain at least in part by Precambrian continental basement [*Li et al.*, 1978; *Yin and Nie*, 1996], although *Sengör and Natal'in* [1996] suggested that it is underlain by Paleozoic arc and accretionary complexes and *Hsü et al.* [1995] concluded that it is

0148-0227/03/2002JB001876$09.00

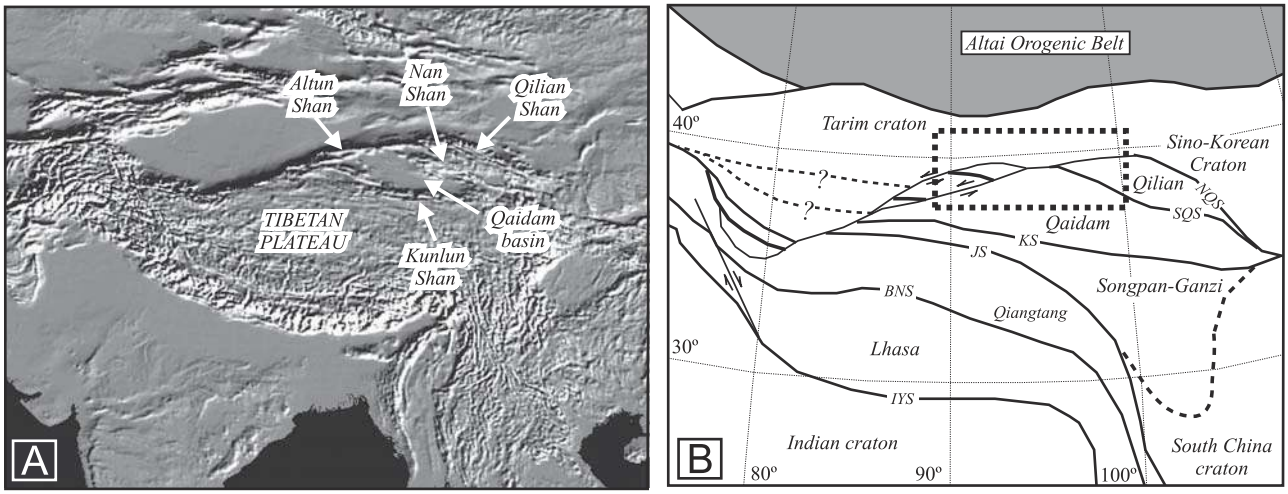

Figure 1. Sketch maps showing (a) location of the Altun Shan, Nan Shan, and Qilian Shan in the northeastern portion of the Tibetan Plateau and (b) location of the study area with respect to the main crustal fragments and sutures in the area. Black dashed box shows the area of Figure 2. Digital topography in Figure 1a is from the GLOBE project of the National Geophysical Data Center (http://www.ngdc.noaa.gov/seg/topo/globe.shtml). Terranes and sutures in Figure 1b are from *Yin and Harrison* [2000]. IYS, Indus-Yalu suture; BNS, Bangong-Nujiang suture; JS, Jinsha suture; KS, Kudi suture; SQS, South Qilian suture; NQS, North Qilian suture.

underlain by Paleozoic oceanic crust that formed in a back arc setting. Resolving between these three possibilities is one of the main objectives of the present study.

[4] According to most previous syntheses, arc-type and oceanic rocks in the northeastern part of the Tibetan Plateau formed within an early Paleozoic convergent margin that was built along or outboard of the southern and southwestern (using present coordinates) margin of the Tarim/Sino-Korean craton [*Li et al.*, 1978; *Hsü et al.*, 1995; *Yin and Nie*, 1996; *Xia et al.*, 1996; *Sengör and Natali'in*, 1996; *Sobel and Arnaud*, 1999; *Xu et al.*, 2000; *Yang et al.*, 2000, 2001; *Yin and Harrison*, 2000]. These syntheses support three fundamentally different models for the main processes by which the arc-type and oceanic terranes were created and eventually accreted.

[5] *Hsü et al.* [1995] proposed that the Tarim/Sino-Korean craton was rimmed to the south by an archipelago of oceanic arcs and back arc basins. This subduction system faced south (dipped north) overall, but collapse of smaller oceanic basins within the archipelago occurred along subduction zones that may have faced south [*Yin and Harrison*, 2000; *Xu et al.*, 2000; *Yang et al.*, 2001], both south and north [*Li et al.*, 1978; *Xiong and Coney*, 1985], or north [*Xia et al.*, 1996]. A second model, proposed by *Sengör and Natal'in* [1996], holds that early Paleozoic magmatism migrated progressively southward from the Tarim/Sino-Korean margin, with magmatic arcs being built on slightly older accretionary complexes. A third model, presented by *Sobel and Arnaud* [1999], suggests that a major mid-Paleozoic suture separates the oceanic terranes from the Tarim/Sino-Korean craton, and that this suture closed along a north facing (south dipping) subduction system. Testing these three models is a second major objective of the present study.

[6] The timing of accretion of arc systems to the Tarim/Sino-Korean craton is relatively well established by the occurrence of Devonian strata that unconformably overlie the older accreted terranes [*Liu*, 1988], and by previous thermochronologic studies. *Sobel and Arnaud* [1999], *Sobel et al.* [2001], and *Delville et al.* [2001] used thermochronologic data from the Altun Shan and nearby ranges to show that a regional metamorphic event occurred in the region between ~435 Ma and ~380 Ma. This metamorphism is interpreted by these workers to record accretion of the arc-type terranes to the Tarim/Sino-Korean craton. A third objective of the present study is to determine the history of magmatism during and immediately prior to this Silurian-Devonian accretionary event.

[7] Following mid-Paleozoic accretion, rocks in the study area have experienced several additional phases of deformation, metamorphism, and uplift. *Sobel et al.* [2001] and *Delville et al.* [2001] present thermochronologic data that record cooling events during late Paleozoic through Late Jurassic time, and the entire region has clearly experienced profound deformation and uplift during Tertiary India-Asia collision. In the study area, Tertiary deformation is clearly evidenced by the abundant thrust faults within the Altun Shan, Nan Shan, and Qilian Shan, and by strike-slip motion on the Altyn Tagh and related faults (Figure 2). These Tertiary tectonic features have been described in considerable detail by *Peltzer and Tapponnier* [1988], *Tapponnier et al.* [1990], *Meyer et al.* [1996], *Métivier et al.* [1998], and *Tapponnier et al.* [2001]. A final objective of the present study is to use the magmatic and geologic records north and south of the Altyn Tagh fault to help constrain the amount of offset on the eastern segment of the fault.

2. Present Study

[8] This study uses U-Pb geochronology to address questions concerning the history of subduction- and accretion-related magmatism in the northeast Tibetan Plateau. Twenty-three samples have been collected and analyzed.

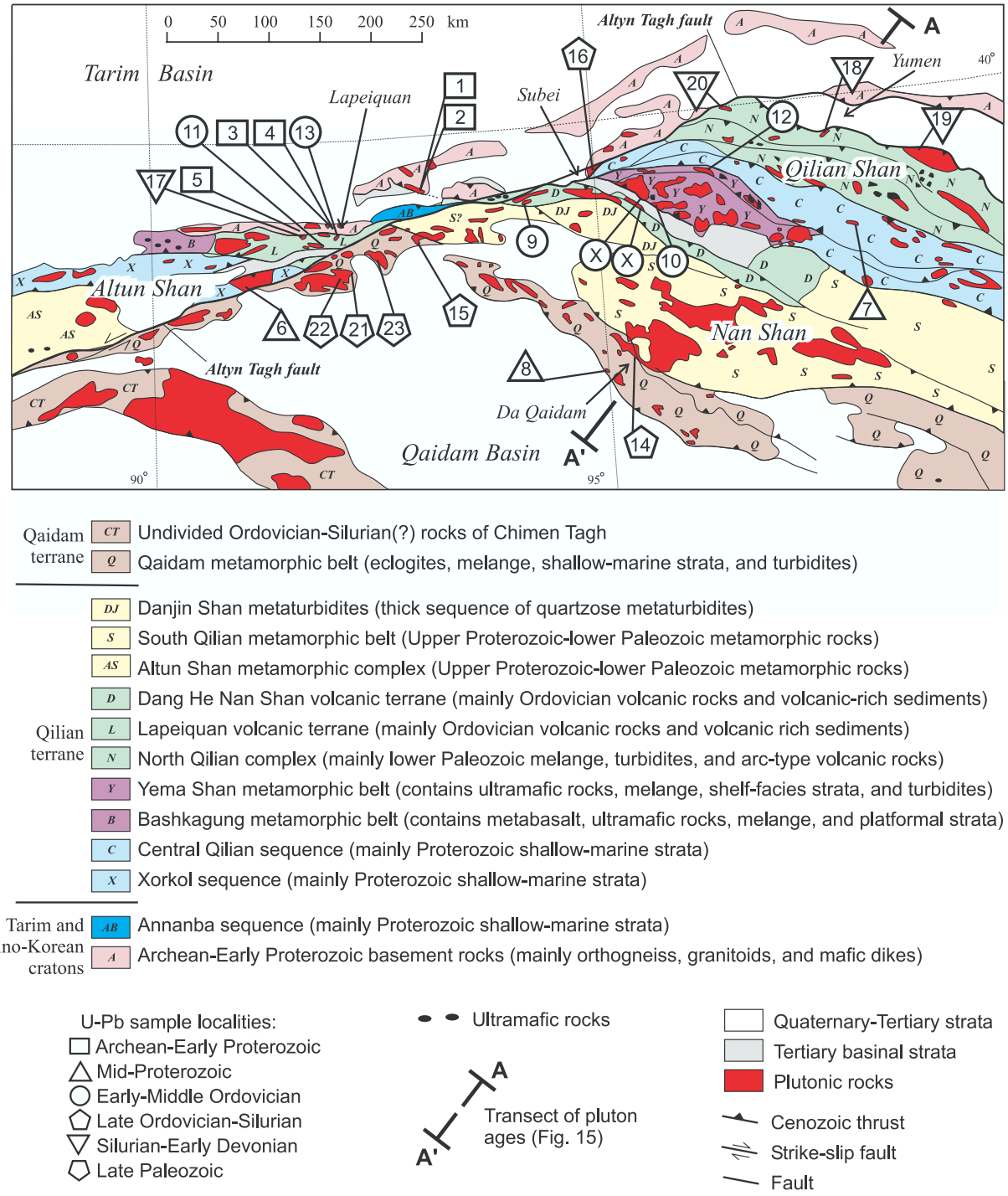

Figure 2. Map of the main tectonic assemblages and first-order structures in the northeastern part of the Tibetan Plateau (adapted from *Liu* [1988]). Geographic names in text and on map are from *U.S. National Imagery and Mapping Agency* [1989]. Terrane names and divisions are adapted from *Yin and Harrison* [2000]. The two Early to Middle Ordovician age samples labeled "X" are from E. Cowgill (written communication, 2002).

The results of our analyses are discussed in the following section, with analytical information presented on Pb/U concordia diagrams, described in Appendix A, and reported in auxiliary material Table A1.[1]

3. Results

3.1. Archean-Early Proterozoic Crystalline Basement

[9] The crystalline basement of the Tarim/Sino-Korean craton is exposed in several isolated areas along the northeastern margin of the Tibetan Plateau [*Liu*, 1988]. Where seen during this study, the basement consists of three main components: layered diorite-quartz diorite gneiss, massive

[1]Supporting tables are available at ftp://agu.org/apend/jb/2002JB001876.

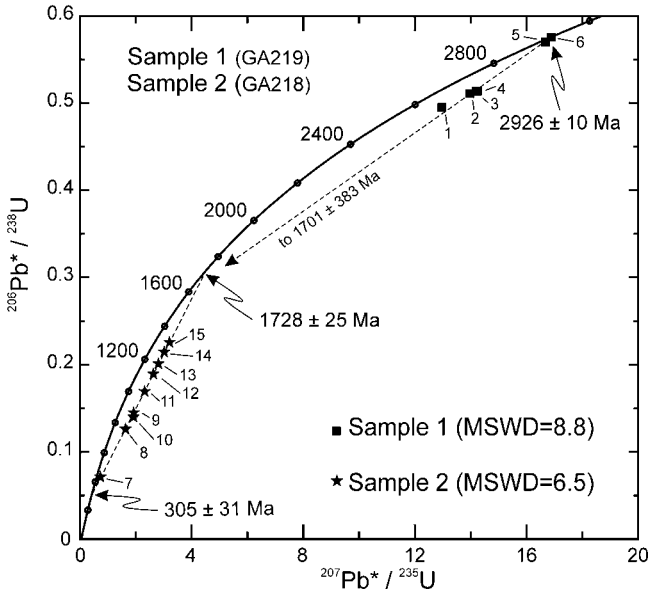

Figure 3. Pb/U concordia diagram of samples 1 and 2. Note that uncertainties in this and following concordia diagrams are at the 95% confidence level. Data reduction and plotting are from programs of *Ludwig* [1991a, 1991b]. The 2926 ± 10 Ma age for sample 1 is interpreted mainly from the $^{207}Pb^*/^{206}Pb^*$ age of a concordant grain (analysis 6 in Table A1), whereas the 1728 ± 25 Ma age for sample 2 is determined from the upper intercept of a discordia through all analyses.

pinkish granite to quartz alkali syenite, and swarms of mafic dikes. This complex is shown on the maps of *Liu* [1988] as Archean/Proterozoic in age, and ages of ~2462 Ma (U-Pb on zircon) and 2787 ± 151 Ma and 2792 ± 208 Ma (Sm-Nd) are reported by *Wang et al.* [1993] and *Che and Sun* [1996]. Our samples have been collected from three areas, as described below and shown on Figure 2.

3.1.1. Sample 1

[10] This sample was collected from a layered diorite-quartz diorite gneiss exposed in a basement uplift within the southern Tarim basin (Figure 2). Six large euhedral crystals were analyzed, four of which were abraded prior to analysis. One of the grains (analysis 6) yields a concordant age of ~2926 Ma, which we interpret as the crystallization age, whereas all of the others are moderately discordant (Figure 3). The discordia has a lower intercept of ~1701 Ma, which presumably records Pb loss during emplacement of granitic dikes that intrude the gneiss (see sample 2 discussion below).

3.1.2. Sample 2

[11] Intrusive into the gneiss described above is a small granite body, which was collected as sample 2. Nine individual grains were analyzed, of which four were abraded. The analyses are all highly discordant, but define a well-constrained discordia with intercepts of 1728 ± 25 Ma and 305 ± 31 Ma. The upper intercept is interpreted as the crystallization age, and the lower intercept is interpreted as the approximate age of Pb loss. A likely interpretation is that Pb loss in the zircons from sample 1 occurred during emplacement of this younger granite, but that zircons in the gneiss were not affected by the ~305 Ma isotopic disturbance. The difference in behavior may result from the higher uranium concentration in the younger zircons from sample 2.

3.1.3. Sample 3

[12] A second sample of quartz dioritic orthogneiss was collected from a small body exposed near the southern margin of Tarim basement in the northeastern Altun Shan (Figure 2). As shown on Figure 4, the grains yield a range of highly discordant ages that do not lie along a simple discordia. The minimum age of the sample is constrained by the $^{207}Pb^*/^{206}Pb^*$ age of the oldest grain, which is ~2642 Ma (Table A1). A possible explanation of the complex discordance pattern relies on U-Pb data from a sample of crosscutting granite (sample 4). As described below, this sample yields a well-defined discordia array with intercepts at 1877 ± 10 Ma and 375 ± 42 Ma, which are interpreted as the ages of crystallization and Pb loss (respectively). These data indicate that the gneiss must be older than ~1877 Ma, and must also have experienced the same isotopic disturbance at ~375 Ma. One possible history, shown on Figure 4, is that the zircons in sample 3 crystallized originally at ~2720 Ma (the upper intercept of the two least-discordant grains), experienced Pb loss (and/or zircon growth) at ~1877 Ma, and were then isotopically disturbed at ~375 Ma.

3.1.4. Sample 4

[13] This sample was collected from a 3-m-wide dike of nonfoliated pinkish leucogranite that intrudes across the foliation and layering of the Archean gneiss described above (sample 3). Eleven single grains were analyzed, of which six were strongly abraded prior to analysis. The analyses define a well-constrained discordia with intercepts of 1877 ± 10 Ma and 375 ± 42 Ma (Figure 3). The upper intercept is interpreted as the age of crystallization, whereas

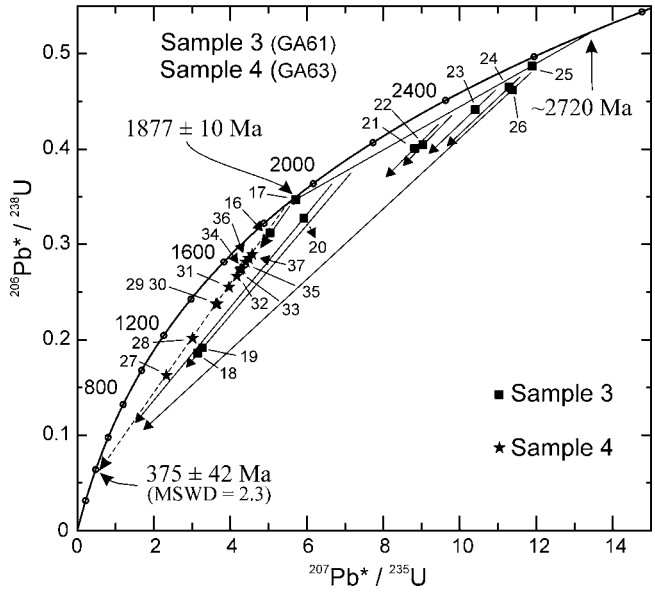

Figure 4. Pb/U concordia diagram of samples 3 and 4. See text for discussion of the possible age for sample 3. The 1877 ± 10 Ma age for sample 4 is determined from the upper intercept of a regression through all of the analyses.

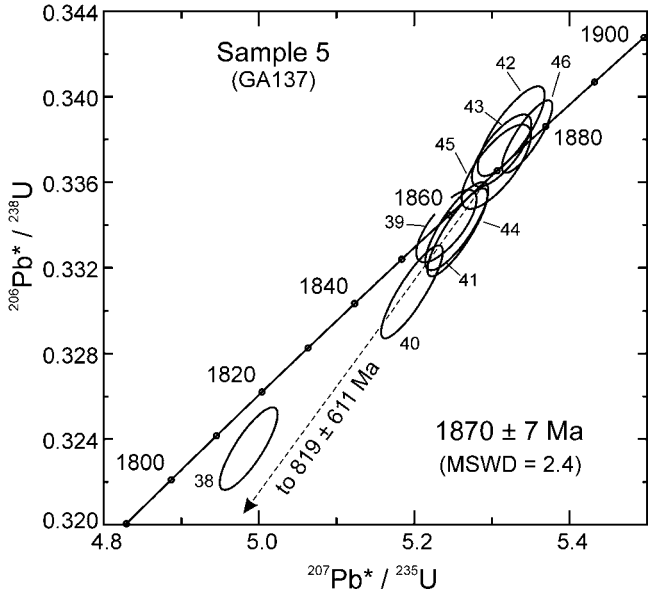

Figure 5. Pb/U concordia diagram of sample 5. The 1870 ± 7 Ma age for this sample is interpreted from the upper intercept of a discordia through all analyses.

the lower intercept apparently records the age of Pb loss and/or new zircon growth.

3.1.5. Sample 5

[14] Sample 5 was collected from a coarse-grained quartz alkali syenite located along the southernmost margin of the Tarim craton in the northeastern Altun Shan (Figure 2). Nine abraded single grains were analyzed (Figure 5). A discordia through these analyses yields an interpreted crystallization age of 1870 ± 7 Ma and a Pb loss age of 819 ± 611 Ma.

3.2. Mid-Proterozoic Plutons

3.2.1. Sample 6

[15] A large body of porphyritic granite that intrudes marble, quartzite, and metapelite of the Xorkol sequence was sampled along the southern margin of the northeastern Altun Shan (Figure 2). Eight single grains were analyzed, of which three were abraded prior to analysis. Five of the grains yield concordant analyses of 922 ± 6 Ma, and two additional analyses define a discordia with an upper intercept (interpreted as the average age of inherited components) of 1884 ± 185 Ma (Figure 6a). An additional grain yields much younger ages, presumably due to Pb loss.

3.2.2. Sample 7

[16] A small granitic pluton that intrudes marble, quartzite, and pelitic schist of the Central Qilian sequence was sampled for U-Pb analysis. Nine single grains were analyzed, all of which were strongly abraded prior to analysis. The analyses range from concordant to moderately discordant, and define a discordia with intercepts of 922 ± 5 Ma and −7 ± 33 Ma (Figure 6b).

3.2.3. Sample 8

[17] This sample comes from a heterogeneous intrusive body located west of the town of Da Qaidam in the western Nan Shan (Figure 2). This body is important because it clearly intrudes into the eclogite-bearing ultramafic rocks in the region [*Yang et al.*, 2001] (Appendix A). Ten abraded

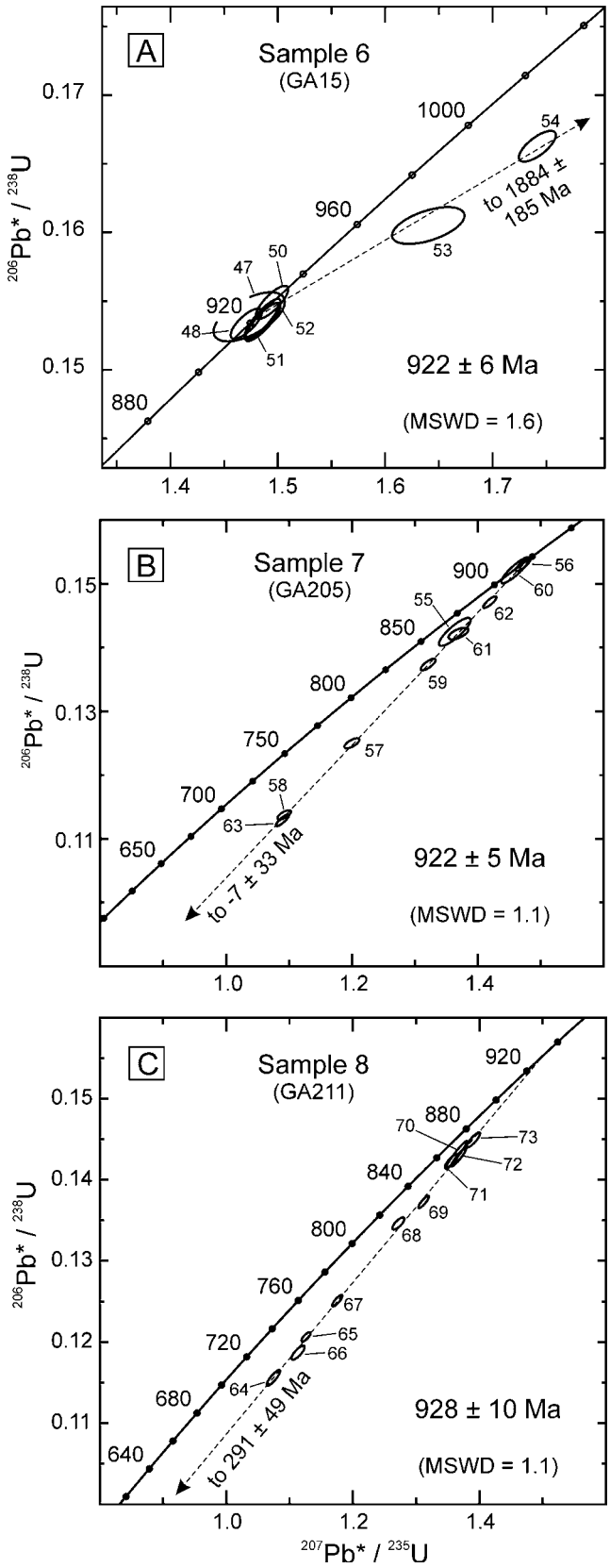

Figure 6. Pb/U concordia diagram of samples (a) 6, (b) 7, and (c) 8. The 922 ± 6 Ma age for sample 6 is interpreted from the cluster of five concordant analyses, whereas the ages of 922 ± 5 Ma for sample 7 and 928 ± 10 Ma for sample 8 are based on regressions through the discordant analyses.

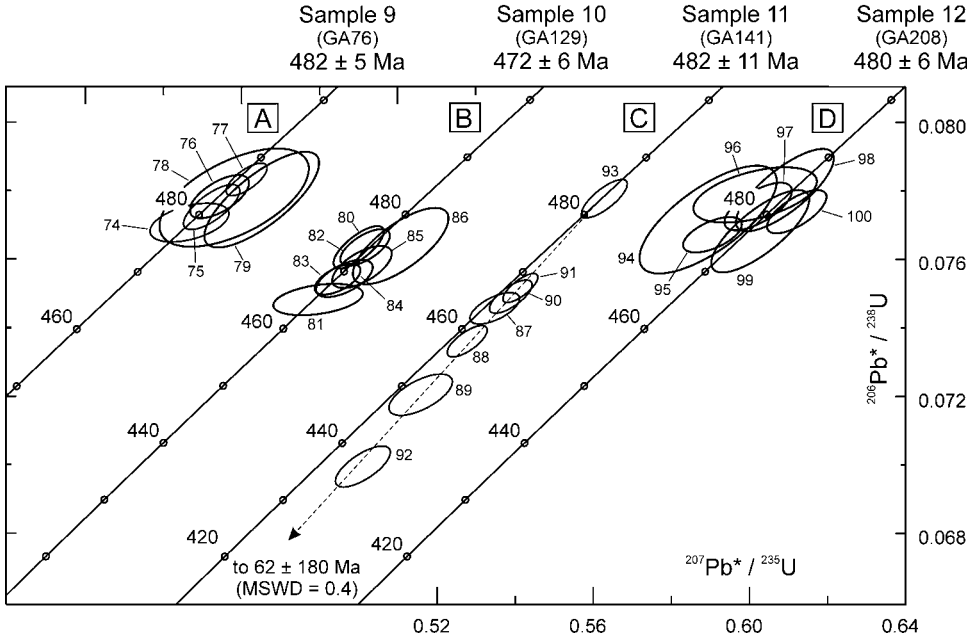

Figure 7. Pb/U concordia diagram of samples (a) 9, (b) 10, (c) 11, and (d) 12. The indicated ages for samples 9, 10, and 12 are based on the clusters of concordant ages, whereas the 482 ± 11 Ma age for sample 11 is based on the upper intercept of a regression through the discordant analyses.

single grains were analyzed, all of which are discordant (Figure 6c). The upper intercept of 928 ± 10 Ma is interpreted as the crystallization age, whereas the lower intercept of 291 ± 49 Ma is interpreted as the age of Pb loss.

3.3. Early to Middle Ordovician Plutons

3.3.1. Sample 9

[18] Intrusive into volcanic and sedimentary rocks of the Dang He Nan Shan volcanic terrane is a nonfoliated quartz diorite pluton (Figure 2). We collected a sample of this pluton from the northwesternmost Nan Shan. Two multigrain fractions and four single grains were analyzed. As shown on Figure 7a, all of the analyses are essentially concordant and yield an age of 482 ± 5 Ma. There is no sign of inheritance or Pb loss.

3.3.2. Sample 10

[19] This sample was collected from a coarse-grained granite located in the Yema Shan metamorphic belt, which is in the northern Nan Shan (Figure 2). Seven individual crystals were analyzed, all of which are concordant at 472 ± 6 Ma (Figure 7b).

3.3.3. Sample 11

[20] A nonfoliated granite body that intrudes volcanic and sedimentary rocks of the Lapeiquan volcanic terrane was sampled in the northeastern Altun Shan (Figure 2). Seven multigrain fractions were analyzed, of which one is apparently concordant and the rest are moderately discordant. A regression through the analyses yields an upper intercept of 482 ± 11 Ma and a lower intercept of 62 ± 180 Ma (Figure 7c). These are interpreted, respectively, as the ages of crystallization and Pb loss.

3.3.4. Sample 12

[21] This sample is from a large body of nonfoliated, medium- to coarse-grained granite that intrudes blueschist-facies metasedimentary and mafic metavolcanic rocks of the Yema Shan metamorphic belt. Seven individual zircon crystals were analyzed, all of which were abraded prior to analysis. The grains are all concordant at 480 ± 6 Ma (Figure 7d).

3.3.5. Sample 13

[22] A sample has also been analyzed from a small body of reddish granite that crops out near the village of Lapeiquan in the northeastern Altun Shan (Figure 2). The body intrudes volcanic and sedimentary rocks of the Lapeiquan volcanic terrane. One multigrain fraction and eleven single grains were analyzed, with abrasion of four

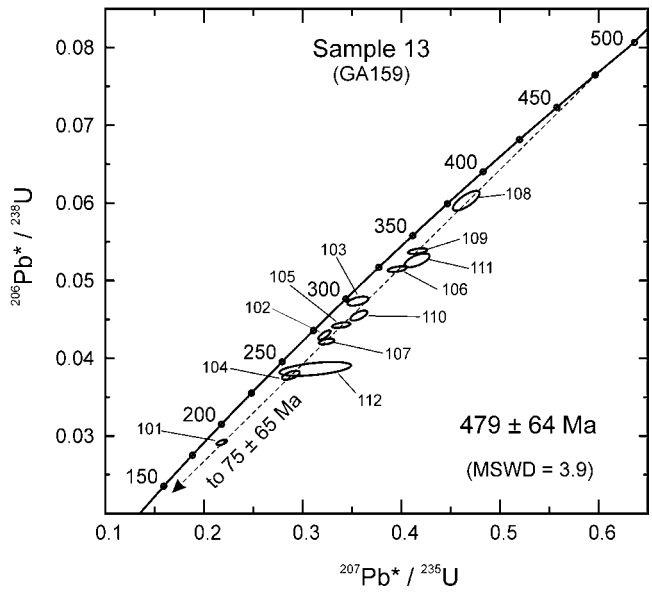

Figure 8. Pb/U concordia diagram of sample 13. This sample yields a very poorly constrained age of 479 ± 64 Ma based on the upper intercept of a regression through the highly discordant analyses.

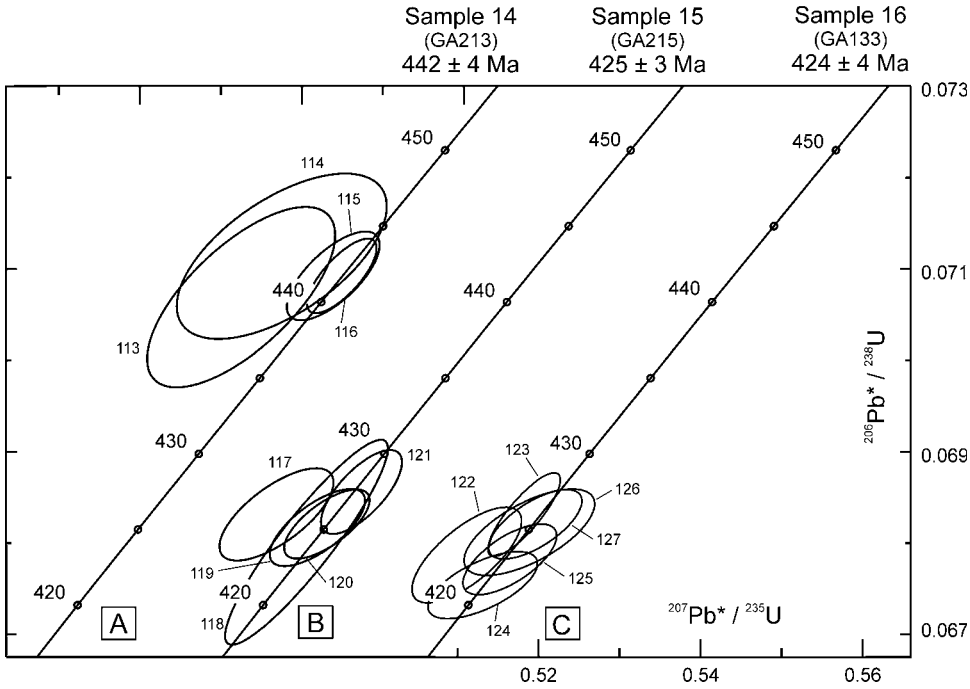

Figure 9. Pb/U concordia diagram of samples (a) 14, (b) 15, and (c) 16. The indicated ages are determined from the clusters of concordant analyses.

larger grains (Table A1). All of the analyses are highly discordant (Figure 8). The upper intercept of 479 ± 64 Ma is interpreted as the approxim ate age of crystallization, whereas the lower intercept of 75 ± 65 Ma is interpreted as the approximate age of Pb loss (Figure 8).

3.4. Late Ordovician-Silurian Plutons With No Inheritance

3.4.1. Sample 14

[23] This sample was collected from a large granite body near the town of Da Qaidam in the western Nan Shan (Figure 2). Four individual zircon crystals were analyzed, all of which overlap at an age of 442 ± 4 Ma (Figure 9a). The shift of two analyses to the left of concordia (Figure 9a) presumably results from low Pb signal intensities (low U concentration) and high common Pb concentrations.

3.4.2. Sample 15

[24] Intrusive into the Qaidam metamorphic belt is a small body of foliated quartz diorite (Figure 2). We sampled this body from the same locality (within ~100 m) that a K-Ar age of 1120 Ma is shown on the geologic map of the area [*Regional Geological Survey Team of Qinghai Bureau of Mines and Geology (RGST-QBMG)*, 1986]. It was hoped that our sample would help constrain the age of Precambrian(?) basement beneath the Qaidam basin. Five zircon crystals were analyzed, all of which are concordant at 425 ± 3 Ma (Figure 9b). The difference between this age and the Precambrian K-Ar age is most likely due to analytical problems with the older data (e.g., excess Ar).

3.4.3. Sample 16

[25] This sample was collected from a large granite body in the northernmost Nan Shan, north of the Altyn Tagh fault (east of the town of Subei) (Figure 2). The granite intrudes metasedimentary and metavolcanic rocks that probably belong to the North Qilian melange complex. Six individual crystals were analyzed, all of which are apparently concordant at 424 ± 4 Ma (Figure 9c). There is no sign of inheritance in the zircons analyzed.

3.5. Silurian-Early Devonian Plutons With Inheritance

3.5.1. Sample 17

[26] This sample was collected from a nonfoliated granite body that occurs along the northern margin of the Lapeiquan volcanic terrane in the Altun Shan (Figure 2). The pluton intrudes metavolcanic and metasedimentary rocks of probable arc affinity, and is structurally juxtaposed against Precambrian basement of the Tarim craton. Four single grains ~80 μ in length were analyzed, as well as three multigrain fractions consisting of three grains ~60 μ in length (Table A1). Two single grains and two multigrain fractions yield concordant analyses, with an age of 413 ± 5 Ma, and additional analyses reveal the presence of inherited components with an average age of ~ 2.1 Ga (Figure 10).

3.5.2. Sample 18

[27] A large body of granite was sampled in the northeasternmost Qilian Shan (Figure 2). The pluton intrudes Paleozoic metasedimentary rocks of the North Qilian complex. Five multigrain fractions and five single grains were analyzed, of which five are concordant and five are moderately to highly discordant (Figure 11). The concordant grains yield an interpreted crystallization age of 406 ± 12 Ma, and the discordant grains contain inherited components of mid-Proterozoic and Late Archean age.

3.5.3. Sample 19

[28] This sample comes from a large granite body in the northeastern Qilian Shan (Figure 2). The body is shown on the map of *Liu* [1988] as intruding sedimentary rocks of Paleozoic age, which we interpret as part of the North Qilian

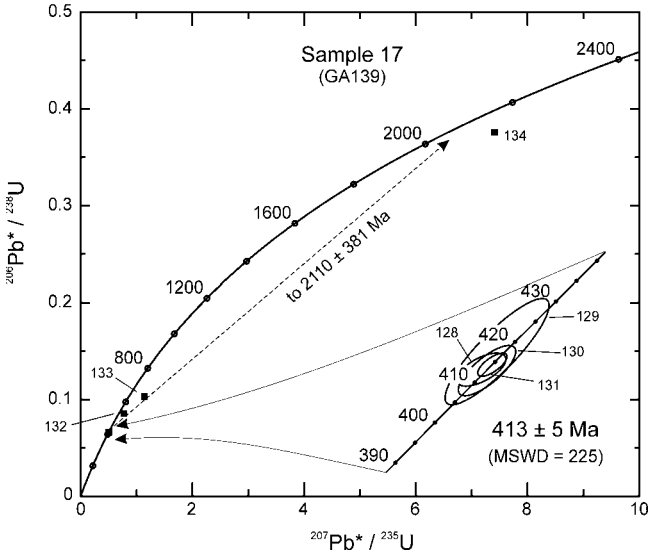

Figure 10. Pb/U concordia diagram of sample 17. The 413 ± 5 Ma age for this sample is determined from the four concordant analyses. The upper intercept of 2110 ± 381 Ma is based on a regression through the discordant analyses and the cluster of concordant analyses.

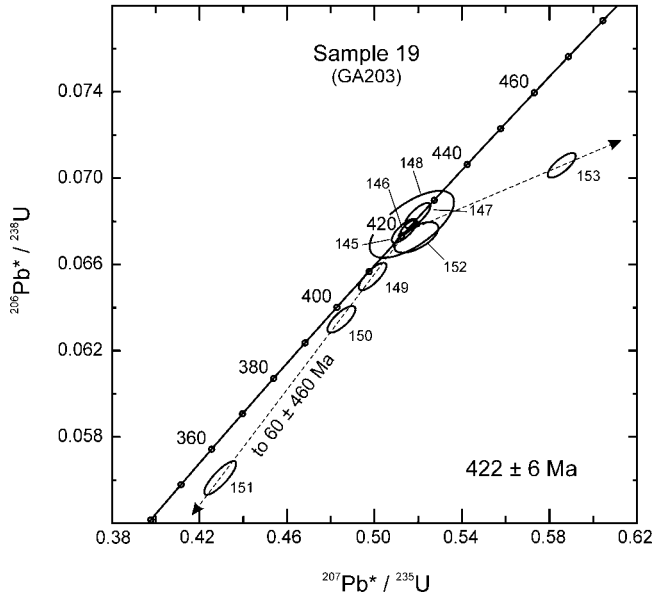

Figure 12. Pb/U concordia diagram of sample 19. The 422 ± 6 Ma age for this sample comes from the cluster of five concordant analyses. A regression line through the oldest grain and the cluster of concordant grains yields an upper intercept of 2446 ± 200 Ma.

complex. Nine single grains were analyzed, of which five are apparently concordant at 422 ± 6 Ma (the interpreted crystallization age) and four are discordant (Figure 12). The discordance pattern suggests that both Pb loss and inheritance are present.

3.5.4. Sample 20

[29] A small granite body was sampled in the northernmost Qilian Shan (Figure 2). The rock intrudes lower Paleozoic volcanic and sedimentary rocks of the North Qilian complex. Six multigrain fractions were analyzed, two of which are nearly concordant and four of which are highly discordant (Figure 13). The lower intercept of 423 ± 6 Ma is interpreted as the age of crystallization, whereas the upper intercept of 1845 ± 86 is interpreted as the average age of inherited components.

3.6. Late Paleozoic Plutons

[30] Samples were collected from plutons along the northern margin of the Qaidam basin in an effort to determine the ages of crystalline basement that extends

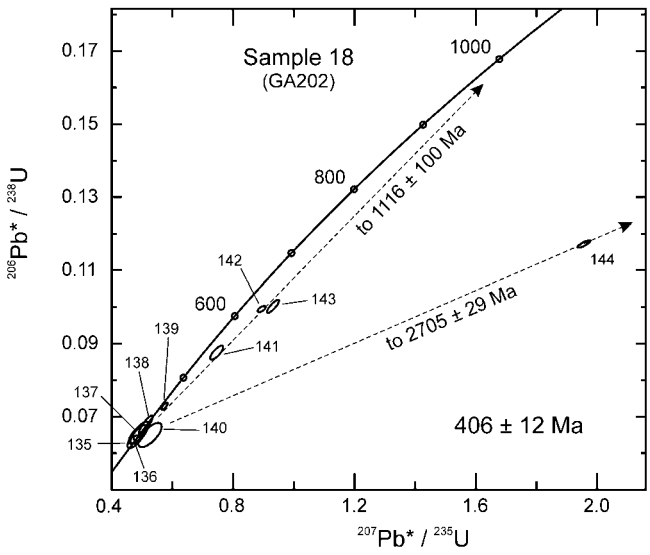

Figure 11. Pb/U concordia diagram of sample 18. The 406 ± 12 Ma age for this sample is derived from the cluster of five concordant analyses. Inherited components have apparent ages of mid-Proterozoic and Late Archean.

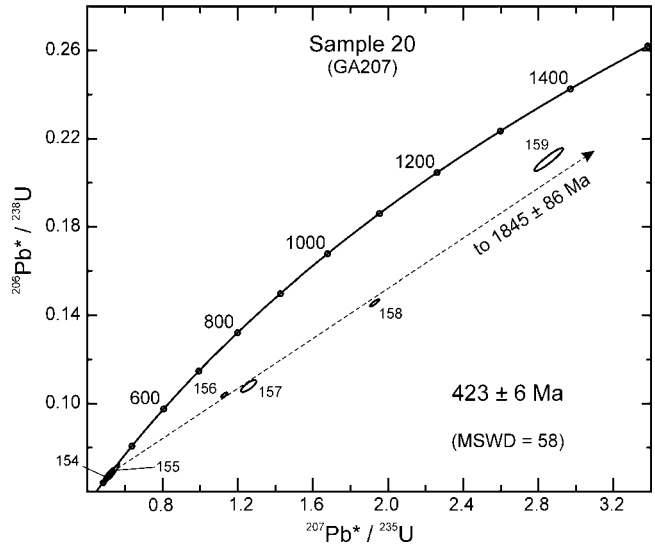

Figure 13. Pb/U concordia diagram of sample 20. The 423 ± 6 Ma age for this sample is determined from the lower intercept of a regression through the discordant analyses. The upper intercept age of 1845 ± 86 Ma is interpreted as the average age of inherited components.

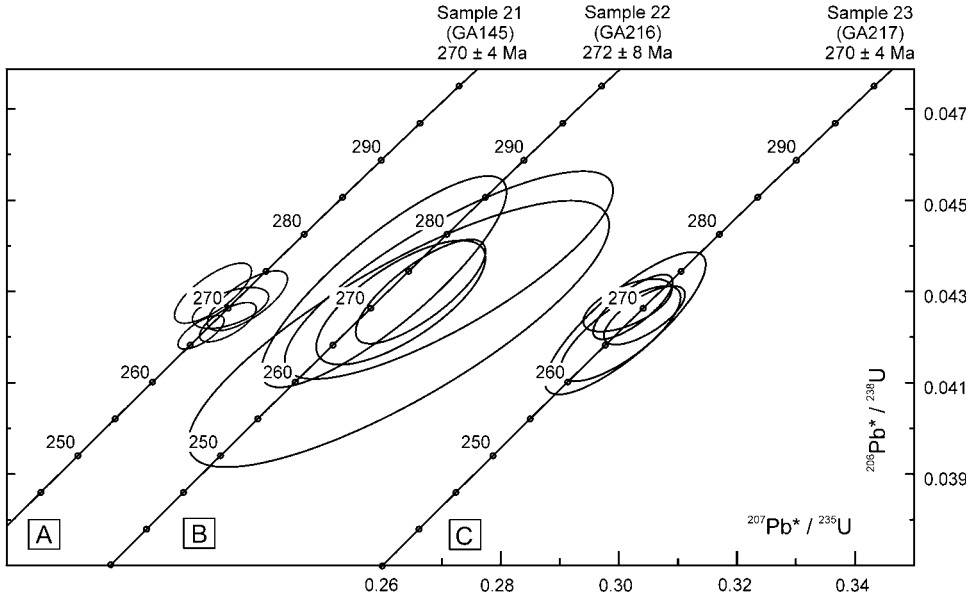

Figure 14. Pb/U concordia diagram of samples (a) 21, (b) 22, and (c) 23. The ages for these three samples come from the clusters of concordant analyses.

beneath the Qaidam basin. Two of the bodies sampled had previously yielded Precambrian K-Ar ages, which provided support for the interpretation that Qaidam is floored by Precambrian basement.

3.6.1. Sample 21

[31] This sample was collected from a medium-grained leucogranite exposed along the north central margin of the Qaidam basin (Figure 2). The pluton intrudes various early Paleozoic(?) diorite and quartz diorite bodies that are exposed along the northern margin of the Qaidam metamorphic belt. Five abraded single grains were analyzed, and all are concordant at 270 ± 4 Ma (Figure 14).

3.6.2. Sample 22

[32] A second sample was collected from an unnamed range along the northern margin of the Qaidam basin (Figure 2). Much of this range is underlain by a large and homogeneous body of nonfoliated quartz diorite. Our sample was collected from the same locality as a K-Ar age of 1474 Ma [*RGST-QBMG*, 1986]. Five single zircon grains were analyzed, all of which are concordant at 272 ± 8 Ma (Figure 14). The relatively low precision of these analyses results from the low U concentration and high common Pb content of the zircon grains.

3.6.3. Sample 23

[33] A third sample from this plutonic suite was collected from the same general region as sample 22 (Figure 2). The body sampled is a quartz diorite layer within a granodiorite-quartz diorite-diorite intrusive complex. A K-Ar age of 794 Ma was reported from the same locality [*RGST-QBMG*, 1986]. Five single zircon grains were analyzed, all of which are concordant at 270 ± 4 Ma (Figure 14).

4. Implications

4.1. Precambrian Rocks of the Tarim/Sino-Korean Craton

[34] Our geochronologic analyses reveal a regionally consistent history of igneous activity for the southern Tarim/Sino-Korean craton. Oldest are layered quartz dioritic-dioritic gneisses that yield Late Archean (2.7–2.9 Ga) crystallization ages. The U-Pb systematics of zircons in these rocks were disturbed during or slightly prior to emplacement of widespread ~1.7–1.9 Ga granitic bodies. Our data record a second phase of isotopic disturbance during mid-Paleozoic time (lower discordia intercepts of ~305 and ~375 Ma for samples 2 and 4). This disturbance apparently involved low-temperature Pb loss, perhaps due to hydrothermal activity, as an $^{40}Ar/^{39}Ar$ (biotite) age from basement rocks near sample 4 [*Sobel and Arnaud*, 1999] indicates that temperatures in these rocks have not surpassed ~300°C since Early Proterozoic time.

[35] Interestingly, there is no sign of early Paleozoic magmatism in the basement complexes that we have studied. Plutons of this age would be expected to occur in these areas according to common models that portray northeast dipping subduction beneath a southwest facing (in present coordinates) magmatic arc developing along the margin of the Tarim/Sino-Korean craton during Ordovician-Silurian time. The lack of evidence for this magmatic arc raises the possibility that subduction occurred mainly along a northeast facing (southwest dipping) convergent margin constructed along the leading edge of the Qilian and Qaidam terranes. The presence of these arc-related assemblages now resting structurally on Tarim/Sino-Korean basement is presumably a result of mid-Paleozoic obduction followed by Tertiary thrusting.

4.2. Precambrian(?) Basement of Qaidam

[36] Previous workers have suggested that the Qaidam basin is underlain by Precambrian continental basement [*Li et al.*, 1978; *Yin and Nie*, 1996], Paleozoic convergent margin assemblages [*Sengör and Natal'in*, 1996], or oceanic crust formed in a Paleozoic back arc basin [*Hsü et al.*, 1995]. The interpretation that Precambrian basement is present is based in part on ~794, ~1120, and ~1474 Ma K-Ar ages from granitoids along the northern margin of the Qaidam basin [*RGST-QBMG*, 1986]. Given that our samples from these same bodies yield ages of ~425 Ma

and ~270 Ma, we have not been able to document the existence of Precambrian basement beneath northern Qaidam. Our ages, combined with the widespread occurrence of arc-type volcanic assemblages in the country rocks to these plutons [*Liu*, 1988], instead support the interpretation that Qaidam is underlain by latest Proterozoic(?)–early Paleozoic convergent margin assemblages [*Sengör and Natal'in*, 1996].

4.3. Mid-Proterozoic Magmatic Activity

[37] The recognition of ~920–930 Ma igneous rocks in the study area has important implications for the tectonic evolution of this part of the Tibetan Plateau. Intrusion of a mid-Proterozoic granitoid into the ultramafic rocks near Da Qaidam (sample 8) is particularly important, as these ultramafic rocks have been interpreted by *Yang et al.* [2001] to record a major early Paleozoic collisional event between the Qaidam and Qilian terranes. Our data indicate instead that high-pressure metamorphism, and hence any collisional events along this boundary, occurred during or prior to mid-Proterozoic time. The early Paleozoic U-Pb and Ar-Ar ages reported by *Yang et al.* [2001] from these rocks may record emplacement of Ordovician plutons that are widespread in the region (e.g., sample 14), rather than the timing of high-pressure metamorphism.

[38] The occurrence of coeval ~920–930 Ma granitoids intrusive into shallow marine strata of the Qilian terrane, as well as into ultramafic rocks of the Qaidam terrane, indicates that much of the region may be underlain by the same mid-Proterozoic and perhaps older basement. On the basis of the lithologic descriptions of *Liu* [1988] and our own mapping, a reasonable scenario is that this basement consists of oceanic assemblages (e.g., slices of oceanic crust, ~920 Ma magmatic arcs(?), thick piles of turbidites, and sequences of shallow marine strata) that were amalgamated into a coherent crustal fragment by mid-Proterozoic time. This crustal fragment apparently did not form in proximity to the Tarim/Sino-Korean craton because (1) there is no evidence of ~920–930 Ma magmatism in the cratonal areas, (2) the shallow marine sedimentary sequences and metaturbidites in the Qilian and Qaidam terranes yield detrital zircon ages that are quite unlike the ages of igneous rocks in the Tarim/Sino-Korean craton [*Gehrels et al.*, 2003], and (3) it is clear from geologic, thermochronologic, and petrologic evidence that the Qilian and Qaidam terranes are separated from the Tarim/Sino-Korean craton by a major mid-Paleozoic suture [*Liu*, 1988; *Sobel and Arnaud*, 1999; *Yang et al.*, 2001].

4.4. Early Paleozoic Magmatic Activity

[39] Early Paleozoic plutons in the study area are emplaced into the mid-Proterozoic and older(?) basement described above, and into lower Paleozoic marine strata, arc-type volcanic rocks, and accretionary complexes. The plutons can be divided into an older suite of dioritic to granitic bodies that occur throughout the study area, and a younger suite of granitic to leucogranitic bodies that occur only along the northeastern margin of the Qilian Shan and Altun Shan (Figure 2).

[40] The older plutons range from ~482 to ~425 Ma (Early Ordovician to mid-Silurian according to the time-scale of *Tucker and McKerrow* [1995]), and E. Cowgill (written communication, 2002) has determined Pb/U ages of ~459 and ~461 Ma on two additional bodies in the central Nan Shan (two samples labeled "X" on Figure 2). These bodies yield zircons that show little evidence of incorporation of older crustal material.

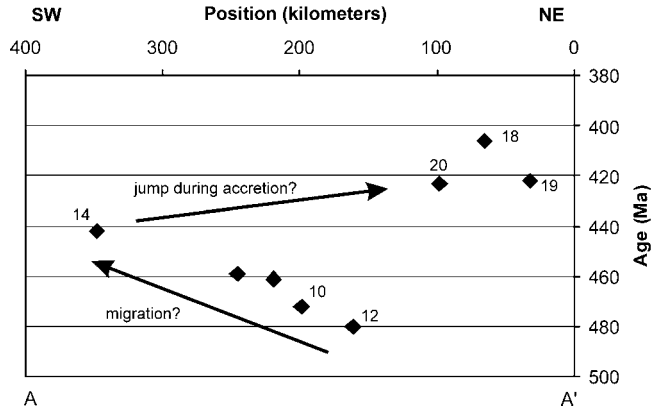

Figure 15. Plot of apparent Pb/U ages of plutons along a northeast-southwest section across the Nan Shan and Qilian Shan (A-A' on Figure 2). Sample numbers are shown for each age, with two additional unlabeled samples from E. Cowgill (written communication, 2002). Samples along the Altyn Tagh fault and in the Altun Shan are not included because of uncertainties in their projected position along the line of section. The southwestward younging from ~480 to ~440 Ma is interpreted as a record of migration of arc magmatism, whereas the northeastward jump between ~440 and ~423 Ma may record the onset of accretion-related crustal melting. Note that uncertainties in age and position are generally smaller than the symbols.

[41] The younger plutons are more felsic in composition (generally granites and leucogranites) and yield zircons that commonly contain significant inherited components. Inheritance ages suggest incorporation of zircons primarily of Late Archean and Early Proterozoic age (Figures 10–13), which is consistent with derivation from the nearby Tarim/Sino-Korean cratonal crust. These bodies yield ages of ~424 Ma to ~406 Ma (mid-Silurian to Early Devonian).

[42] A plot of Pb/U ages along a northeast-southwest line of section across the Qilian Shan and Nan Shan (Figure 15) emphasizes the spatial difference between the older and younger suites of plutons, and also suggests that magmatism migrated southwestward between ~480 Ma and ~440 Ma. The same southward younging trend is also apparent in ages of plutons in the Altun Shan and along the Altyn Tagh fault, but these ages are not shown on Figure 15 because of uncertainties in their projected paleoposition along the line of section.

[43] The patterns of early Paleozoic plutonism in the region, combined with the constraints derived from geochronologic studies of Precambrian rocks in the region, as outlined above, yield the preferred model shown in Figure 16. Following *Sobel and Arnaud* [1999], we suggest that Ordovician-Early Silurian magmatism in the region occurred in a northeast facing magmatic arc that formed in response to southwest

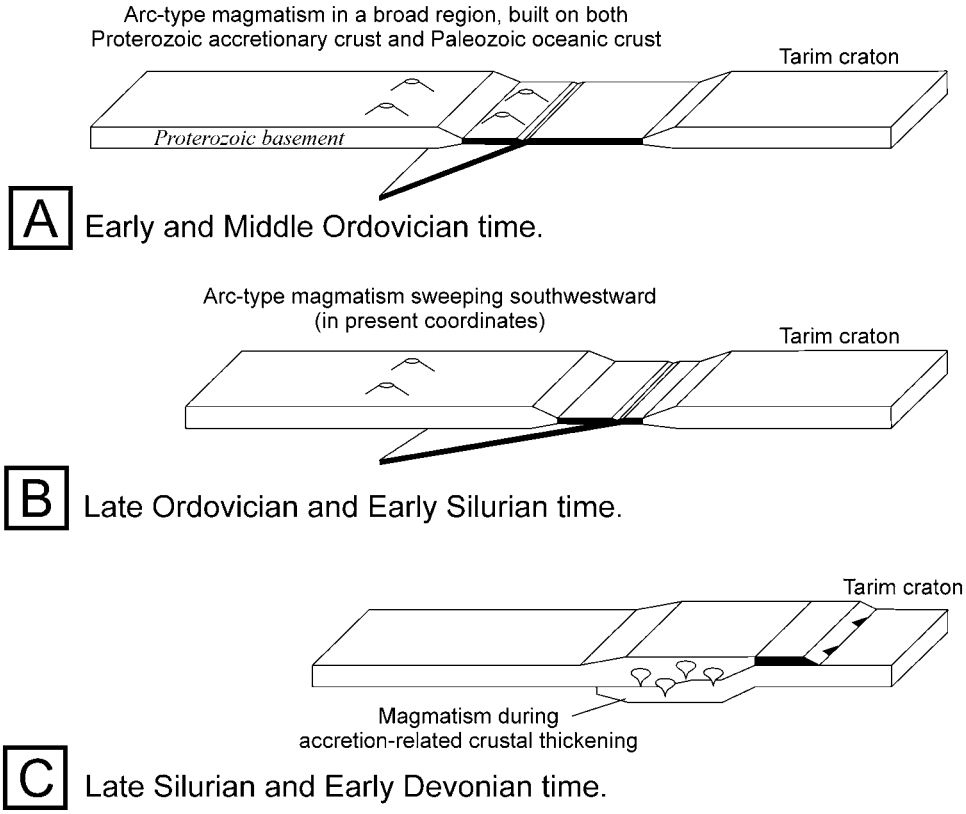

Figure 16. Proposed model for the tectonic setting of magmatism in the northeastern Tibetan Plateau during early Paleozoic time. This model is consistent with views of *Sobel and Arnaud* [1999] but differs from most previous scenarios in that (1) the main subduction system is interpreted to have dipped southwest rather than northeast and (2) the Ordovician-Silurian magmatic arcs are interpreted to have been built on mid-Proterozoic basement that was not originally tied to Tarim/Sino-Korean craton.

dipping subduction along the leading edge of the composite Qilian-Qaidam terrane. Our Pb/U data suggest that magmatism migrated southwestward between ~480 and ~440 Ma, perhaps through changes in subduction geometry, and then jumped northeastward at ~425 Ma during the onset of collisional accretion of the Qilian-Qaidam terrane to the Tarim/Sino-Korean craton.

[44] The age of onset of accretion is constrained with relatively high precision. $^{40}Ar/^{39}Ar$ (biotite) analyses from plutonic rocks in the Altun Shan yield ages of ~453 and ~431 Ma for premetamorphic plutons, ~432 and ~414 Ma for syntectonic intrusions, and ~383 Ma for a posttectonic leucogranite [*Sobel and Arnaud*, 1999]. Along our northeast-southwest transect (Figure 15), the change is bracketed between 442 ± 4 Ma (sample 14) and 423 ± 6 Ma (sample 20). This can be refined, however, by a pluton in the northern Nan Shan (sample 15) that belongs to the older group and yields an age of 425 ± 3 Ma. The onset of accretion, as recorded by an apparent change from subduction- to accretion-related magmatism, is accordingly bracketed between 425 ± 3 Ma and 423 ± 6 Ma.

[45] Our proposed model differs from the models of *Hsü et al.* [1995] and *Sengör and Natal'in* [1996] primarily in the age of assembly of the crust upon which the early Paleozoic arcs were built. We agree with these authors that crust in the Qaidam and Qilian terranes comprises accretionary complex, magmatic arc, and ocean floor assemblages, but we conclude that crustal assembly occurred during mid-Proterozoic rather than early Paleozoic time.

4.5. Location of Mid-Paleozoic Suture and Implications for Offset on the Eastern Altyn Tagh Fault

[46] Our interpretation of the magmatic history of the region, as summarized on Figure 16, suggests that the fundamental suture separating the Qilian terrane from the Tarim/Sino-Korean craton lies along the northeastern margin of the North Qilian complex in the Qilian Shan (Figure 2). The equivalent boundary north of the Altyn Tagh fault would trace along the northern margin of the Lapeiquan volcanic terrane in the eastern Altun Shan, as suggested by *Sobel and Arnaud* [1999]. Correlation of these features, as well as the North Qilian and Central Qilian terranes (south of the fault) with the Lapeiquan and Xorkol terranes (north of the fault) (Figure 2), suggests that the eastern Altyn Tagh fault has ~375 km of offset. This is similar to the 350–400 km offset estimates reported by *Molnar and Tapponnier* [1975], *Ritts and Biffi* [2000, 2001], *Sobel et al.* [2001], *Yang et al.* [2001], and *Yue et al.* [2001].

4.6. Late Paleozoic Plutons

[47] The ~270 Ma plutons in the study area are almost certainly related to the widespread late Paleozoic magmatism in the Kunlun Shan, located along the southern margin of the Qaidam basin (Figure 1). Recognition of these ages in

the northern Qaidam basin area suggests that this south facing late Paleozoic arc system was nearly 400 km wide, and/or that considerable tectonic reorganization of the arc has occurred since late Paleozoic time.

5. Conclusions

[48] U-Pb geochronologic data from plutonic rocks in the Nan Shan, Qilian Shan, and Altun Shan provide important constraints on the tectonic evolution of the northeastern portion of the Tibetan Plateau. Conclusions of regional tectonic significance are outlined below.

[49] 1. Our data do not support pre-mid-Paleozoic connections between the Tarim/Sino-Korean craton to the north and east and rocks within the Qilian Shan, Nan Shan, and Altun Shan. The oldest igneous rocks recognized in the terranes to the southwest are mid-Proterozoic in age, and there is little sign of inheritance of older zircons in any of the pre-425 Ma plutons. In addition, we have found no evidence for plutons of mid-Proterozoic to mid-Paleozoic age within cratonal regions to the northeast. Hence our data do not support previous models in which rocks presently in the Altun Shan, Nan Shan, and Qilian Shan originally formed along the southwest margin of the Tarim/Sino-Korean craton. Rather, we follow *Sobel and Arnaud* [1999] in concluding that a major mid-Paleozoic suture separates the Qilian and Qaidam terranes from the Tarim/Sino-Korean craton.

[50] 2. Much of the crust in the Qilian and Qaidam terranes appears to have been assembled prior to emplacement of ~920–930 Ma granitoids. This crust consists largely of slices of oceanic crust, accretionary complexes, volcanic sequences that may have formed in magmatic arcs, thick piles of turbidites, and sequences of shallow marine strata. Some ultramafic rocks contain eclogite-facies assemblages that record collisional events [*Yang et al.*, 2001].

[51] 3. Our geochronologic data are strongly supportive of previous interpretations that arc-type igneous rocks of Ordovician-Silurian age make up much of the Qilian Shan, Nan Shan, and Altun Shan. This magmatism occurred mainly between ~480 Ma and ~425 Ma, and appears to have migrated from northeast to southwest during this time (Figure 15). The pattern of magmatism, combined with the recognition of continuity of Qaidam-Qilian basement and the presence of a major suture along the leading edge of the Qilian terrane, suggests that this magmatism occurred in a northeast facing magmatic arc, resulting from southwest dipping subduction, as suggested previously by *Xia et al.* [1996] and *Sobel and Arnaud* [1999]. This is in contrast to the southwest facing arc polarity described in most syntheses of the early Paleozoic tectonic development of the region.

[52] 4. The early Paleozoic magmatic arc built on the Qilian and Qaidam terranes is interpreted to have collided with the southern margin of the Tarim/Sino-Korean craton during Silurian-Early Devonian time, as has been described by many previous workers. This collisional event is recorded in the igneous record by a northeastward jump in the locus of magmatism (Figure 15), a change to more felsic composition of the plutons, and the occurrence of abundant Archean-Early Proterozoic inherited zircons in the plutons. The change from subduction- to collision-related magmatism is tightly constrained by our data to the interval between 425 ± 3 Ma and 423 ± 6 Ma.

[53] 5. Comparison of the magmatic history in the Altun Shan with that in the Qilian Shan and Nan Shan suggests that the eastern Altyn Tagh fault has a total of ~375 km of offset, which is similar to values proposed by *Molnar and Tapponnier* [1975], *Ritts and Biffi* [2000, 2001], *Sobel et al.* [2001], *Yang et al.* [2001], and *Yue et al.* [2001].

Appendix A: Analytical Methods and Information About Geochronologic Samples

[54] Each sample consisted of ~5 kg of fresh rock collected from a single outcrop. Zircon extraction was conducted in the field using a portable rock grinder (steel pestle that rotates in a steel mortar, powered by a chainsaw motor) to break the rocks into sand-size material, disposable sieve screen to remove rock fragments, and a gold pan to concentrate the heavy minerals. Final mineral separation was accomplished with heavy liquids and a magnetic separator at the University of Arizona, as described by *Gehrels* [2000]. For many samples, the zircons were abraded with an air abrasion device [*Krogh*, 1982] in order to remove outer portions of grains that are more susceptible to Pb loss. Procedures for zircon dissolution, chemical separation, and thermal ionization mass spectrometry are described by *Gehrels* [2000]. Data reduction and plotting was accomplished using programs of *Ludwig* [1991a, 1991b]. All uncertainties are reported at the 95% confidence level.

A1. Sample 1

[55] Most exposures of gneiss at the sample 1 locality display a well-developed foliation that is consistently parallel with the gneissic compositional layering. In most layers, however, a primary igneous texture is preserved. A leucocratic phase of the quartz diorite component was collected. Zircons from the sample are translucent, colorless to light pink, euhedral crystals. The dark pink colors present in zircons from the other Precambrian samples in this study are lacking, presumably due to the low uranium concentration of the grains in this sample (Table A1).

A2. Sample 2

[56] Sample 2 was collected from a small granitic body that is nondeformed and clearly intrudes across the compositional layering and foliation in the older gneiss (sample 1). Zircons in the sample are tan to pinkish in color and euhedral in morphology, and many grains are cloudy due to radiation damage.

A3. Sample 3

[57] The quartz diorite sampled is interlayered with dioritic rocks, and both have a strongly developed foliation and are pervasively folded. The gneiss is intruded by dikes and small stocks of pinkish granite (sample 4), and both are intruded by swarms of mafic dikes. Zircons from the sample are euhedral, with few inclusion and fractures, and range from light to medium pink in color.

A4. Sample 4

[58] Sample 4 yields zircons that are light to medium pink in color, euhedral, and relatively free of fractures and inclusions. Some grains are cloudy and grayish.

A5. Sample 5

[59] Sample 5 was collected from a pluton that occurs immediately below a south dipping fault which juxtaposes early Paleozoic plutons (see sample 15) and associated arc-type volcanic rocks to the south over Tarim basement to the north (Figure 2). Zircons from sample 5 are pinkish in color, euhedral in morphology, and free of inclusions, but they tend to have abundant fractures.

A6. Sample 6

[60] The rock from which sample 6 was collected has a strong foliation and is commonly schistose and locally mylonitic. The presence of potassium feldspar megacrysts up to 5 cm across is a distinctive feature of this rock. Zircons from the sample are generally colorless to light pink in color, and most grains are euhedral in morphology.

A7. Sample 7

[61] The body from which sample 7 was collected occurs along the west flank of the Tulai Nan Shan, which is located in the north central Qilian Shan (Figure 2). The granite has only a moderate foliation and lineation. Zircons in the sample range from colorless to medium pink and commonly are well-formed euhedral crystals.

A8. Sample 8

[62] The sampled plutonic complex is quite variable in composition, ranging from leucogranite to diorite, and is also variable in grain size and texture. Dikes of the body clearly intrude into ultramafic rocks, amphibolite, and eclogite of the Luliang Shan ultramafic complex (part of the Qaidam metamorphic belt, Figure 2), and xenoliths of the ultramafic rocks are widespread in the intrusive body. Similar intrusive relations have been described by *Songnian et al.* [1999]. The component sampled is medium-grained quartz diorite that has a moderately developed foliation. Zircons from the body are clear and colorless, with few inclusions and fractures.

A9. Sample 9

[63] Zircons from sample 9 are colorless and euhedral, with few inclusions and fractures.

A10. Sample 10

[64] The sampled granite intrudes across the foliation in schistose dioritic rocks and does not contain a foliation. Zircons from the sample are colorless and euhedral and have few inclusions and fractures.

A11. Sample 11

[65] Zircons from sample 11 are colorless and euhedral, and most are smaller than 100 μm in sieve size.

A12. Sample 12

[66] Sample 12 was collected from the west flank of the northern Daxue Shan, which is located in the northwestern Qilian Shan (Figure 2). Zircons from the granite are colorless, euhedral, and free of inclusions and fractures.

A13. Sample 13

[67] The sampled rock is highly fractured and altered, presumably due to the numerous faults and widespread hydrothermal activity in the area. Zircons in the sample are colorless to light pink in color, most of the larger grains contain numerous fractures, and many grains are grayish and cloudy.

A14. Sample 14

[68] The sampled body intrudes metasedimentary rocks of the South Qilian metamorphic belt. Zircons from this sample are colorless and euhedral.

A15. Sample 15

[69] Zircons from sample 15 are clear and colorless and contain few inclusions and fractures.

A16. Sample 16

[70] The sampled rock is homogeneous in composition and does not contain a discernible foliation. Zircons from the sample are brown to pink in color and euhedral and tend to be fairly high in uranium concentration (Table A1).

A17. Sample 17

[71] Zircons from this body tend to be light pink in color and euhedral in morphology. The zircons are smaller than is common for a granite, with all grains <100 μm in length.

A18. Sample 18

[72] Zircons from sample 18 are all very small, < 100 μm in length, and most are colorless and euhedral.

A19. Sample 19

[73] Zircons from sample 19 are colorless, euhedral, and relatively small in size (all < 150 μm).

A20. Sample 20

[74] Zircons from sample 20 are colorless, euhedral, and very small (no grains larger than 70 μm are present).

A21. Sample 21

[75] Zircon grains from sample 21 are all colorless and euhedral, with few fractures and inclusions.

A22. Sample 22

[76] Zircons from sample 22 are colorless and euhedral.

A23. Sample 23

[77] Zircons from sample 23 are colorless and euhedral.

[78] **Acknowledgments.** This research was conducted as part of a collaborative project between the University of Arizona; the University of California, Los Angeles; Arizona State University; and the Institute of Geomechanics in Beijing. Funding was provided by the Continental Dynamics Program of the National Science Foundation (EAR-9725663). We thank Robert Butler, Guillaume Dupont-Nivet, and Chen Xunhua for their assistance in the field and Eric Cowgill, Paul Kapp, Brad Ritts, and Steve Graham for helpful discussions about the geology of the region. Reviewed by E. Cowgill and an anonymous reviewer.

References

Che, Z., and Y. Sun, The age of the Altun granulite facies complex and the basement of the Tarim basin, *Reg. Geol. China*, *56*, 51–57, 1996.

Delville, N., N. Arnaud, J.-M. Montel, F. Roger, M. Brunel, P. Tapponnier, and E. Sobel, Paleozoic to Cenozoic deformation along the Altyn Tagh fault in the Altun Shan massif area, eastern Qilian Shan, northeastern Tibet, China, in *Paleozoic and Mesozoic Tectonic Evolution of Central Asia: From Continental Assembly to Intracontinental Deformation*, edited by M. S. Hendrix and G. A. Davis, *Mem. Geol. Soc. Am.*, *194*, 269–292, 2001.

Gehrels, G. E., Introduction to detrital zircon studies of Paleozoic and Triassic strata in western Nevada and northern California, in *Paleozoic and Triassic Paleogeography and Tectonics of Western Nevada and Northern California*, edited by M. J. Soreghan and G. E. Gehrels, *Spec. Pap. Geol. Soc. Am.*, *347*, 1–17, 2000.

Gehrels, G. E., A. Yin, and X.-F. Wang, Detrital zircon geochronology of the northeastern Tibetan Plateau, *Geol. Soc. Am. Bull.*, in press, 2003.

Hsü, K. J., P. Guitang, and A. M. C. Sengör, Tectonic evolution of the Tibetan Plateau: A working hypothesis based on the archipelago model of orogenesis, *Int. Geol. Rev.*, *37*, 473–508, 1995.

Krogh, T. E., Improved accuracy of U-Pb zircon ages by the creation of more concordant systems using an air abrasion technique, *Geochim. Cosmochim. Acta*, *46*, 637–649, 1982.

Li, C. Y., Y. Liu, B. C. Zhu, Y. M. Feng, and H. C. Wu, Structural evolution of Qinling and Qilian Shan, in *Scientific Papers in Geology and International Exchange*, pp. 174–197, Geol. Publ. House, Beijing, 1978.

Liu, Z. Q., Geologic map of the Qinghai-Xizang (Tibet) Plateau and adjacent areas, scale 1:1,500,000, Chengdu Inst. of Geol. and Miner. Resour., Beijing, 1988.

Ludwig, K. R., A computer program for processing Pb-U-Th isotopic data, *U.S. Geol. Surv. Open File Rep.*, 88–542, 1991a.

Ludwig, K. R., A plotting and regression program for radiogenic-isotopic data, *U.S. Geol. Surv. Open File Rep.*, 91–445, 1991b.

Métivier, F., Y. Gaudemer, P. Tapponnier, and B. Meyer, Northeastward growth of the Tibet Plateau deduced from balanced reconstructions of two depositional areas: The Qaidam and Hexi Corridor basins, China, *Tectonics*, *17*, 823–842, 1998.

Meyer, B., P. Tapponnier, Y. Gaudemer, G. Peltzer, S. Guo, and Z. Chen, Rate of left-lateral movement along the easternmost segment of the Altyn Tagh fault, east of 96°E (China), *Geophys. J. Int.*, *124*, 29–44, 1996.

Molnar, P., and P. Tapponier, Cenozoic tectonics of Asia: Effects of a continental collision, *Science*, *189*, 419–426, 1975.

Peltzer, G., and P. Tapponnier, Formation and evolution of strike-slip faults, rifts, and basins during India-Asia collision: An experimental approach, *J. Geophys. Res.*, *93*, 15,085–15,117, 1988.

Regional Geological Survey Team of Qinghai Bureau of Mines and Geology (RGST-QBMG), Eboliang geologic map (J-46–9), scale 1:200,000, Qinghai Prov. Reg. Geol. Surv., Xining, China, 1986.

Ritts, B. D., and U. Biffi, Magnitude of post-Middle Jurassic (Bajocian) displacement on the Altyh Tagh fault, NW China, *Geol. Soc. Am. Bull.*, *112*, 61–74, 2000.

Ritts, B. D., and U. Biffi, Mesozoic northeast Qaidam basin: Response to contractional reactivation of the Qilian Shan, and implications for the extent of Mesozoic intracontinental deformation in central Asia, in *Paleozoic and Mesozoic Tectonic Evolution of Central Asia: From Continental Assembly to Intracontinental Deformation*, edited by M. S. Hendrix and G. A. Davis, *Mem. Geol. Soc. Am.*, *194*, 293–316, 2001.

Sengör, A. M. C., and B. A. Natal'in, Paleotectonics of Asia: Fragments of a synthesis, in *The Tectonics of Asia*, edited by A. Yin and T. M. Harrison, pp. 486–640, Cambridge Univ. Press, New York, 1996.

Sobel, E. R., and N. Arnaud, A possible middle Paleozoic suture in the Altun Shan, NW China, *Tectonics*, *18*, 64–74, 1999.

Sobel, E. R., N. Arnaud, M. Jolivet, B. D. Ritts, and M. Brunel, Jurassic to Cenozoic exhumation history of the Altyn Tagh range, northwest China, constrained by $^{40}Ar/^{39}Ar$ and apatite fission track thermochronology, in *Paleozoic and Mesozoic Tectonic Evolution of Central Asia: From Continental Assembly to Intracontinental Deformation*, edited by M. S. Hendrix and G. A. Davis, *Mem. Geol. Soc. Am.,*, *194*, 247–267, 2001.

Songnian, L., Z. Fengqing, M. Hualin, Y. Haifeng, L. Huaikun, and Z. Jiankang, Discovery and significance of eclogite-granite belts in northwest China, *Gondwana Res*, *2*, 137–138, 1999.

Stacey, J. S., and J. D. Kramers, Approximation of terrestrial lead isotope evolution by a two-stage model, *Earth Plan. Sci. Lett.*, *26*, 207–221, 1975.

Tapponnier, P., et al., Active thrusting and folding in the Qilian Shan, and decoupling between upper crust and mantle in northeastern Tibet, *Earth Planet. Sci. Lett.*, *97*, 382–403, 1990.

Tapponnier, P., X. Zhiqin, F. Roger, B. Meyer, N. Arnaud, G. Wittlinger, and Y. Jingsui, Oblique stepwise rise and growth of the Tibet Plateau, *Science*, *294*, 1671–1677, 2001.

Tucker, R. D., and W. S. McKerrow, Early Paleozoic chronology: A review in light of new U-Pb zircon ages from Newfoundland and Britain, *Can. J. Earth Sci.*, *32*, 368–379, 1995.

U.S. National Imagery and Mapping Agency, Tactical pilotage charts TPC G-8A and G-8B, scale 1:500,000, Bethesda, Md., 1989.

Wang, G. P., G. T. Wu, Z. Q. Lun, and Y. Y. Zhu, Regional Geology of Xinjiang Uygur Autonomous Region, *Geol. Mem., Ser. 1*, vol. 32, 841, Geol. Publ. House, Beijing, 1993.

Xia, L., Z. Xia, and X. Xu, *Origin of the Oceanic Island Arc System in the Northern Qilian Shan*, 153 pp., Geol. Publ. House, Beijing, 1996.

Xiong, J., and P. J. Coney, Accreted terranes of China, in *Tectonostratigraphic Terranes of the Circum-Pacific Region, Earth Sci. Ser.*, vol. 1, edited by D. G. Howell, pp. 349–361, Circum-Pac. Counc. for Energy and Miner. Resour., Houston, Tex., 1985.

Xu, Z., J. Zhang, and H. Li, Architecture and orogeny of the northern Qilian orogenic belt, northwestern China, *J. Geol. Soc. China*, *43*, 125–141, 2000.

Yang, J., Z. Xu, H. Li, C. Wu, J. Zhang, and R. Shi, A Caledonian convergent border along the southern margin of the Qilian terrane, NW China: Evidence from eclogite, garnet-peridotite, ophiolite, and S-type granite, *J. Geol. Soc. China*, *43*, 142–160, 2000.

Yang, J., Z. Xu, J. Zhang, C.-Y. Chu, R. Zhang, and J. G. Liou, Tectonic significance of early Paleozoic high-pressure rocks in Altun-Qaidam-Qilian Mountains, northwest China, in *Paleozoic and Mesozoic Tectonic Evolution of Central Asia: From Continental Assembly to Intracontinental Deformation*, edited by M. S. Hendrix and G. A. Davis, *Mem. Geol. Soc. Am.*, *194*, 151–170, 2001.

Yin, A., and T. M. Harrison, Geologic evolution of the Himalayan-Tibetan orogen, *Annu. Rev. Earth Planet. Sci.*, *28*, 211–280, 2000.

Yin, A., and S. Nie, A Phanerozoic palinspastic reconstruction of China and its neighboring regions, in *The Tectonics of Asia*, edited by A. Yin and T. M. Harrison, pp. 442–485, Cambridge Univ. Press, New York, 1996.

Yue, Y., B. D. Ritts, and S. A. Graham, Initiation and long-term slip history of the Altyn Tagh fault, *Int. Geol. Rev.*, *43*, 1–7, 2001.

G. E. Gehrels, Department of Geosciences, University of Arizona, Tucson, AZ 85721, USA. (ggehrels@geo.arizona.edu)

X.-F. Wang, Chinese Academy of Geological Sciences, Institute of Geomechanics, Beijing, China 100081.

A. Yin, Department of Earth and Space Sciences, University of California, Los Angeles, CA 90095-1567, USA. (yin@ess.ucla.edu)